

The Origin and Formation Mechanism of an Inclined Line-like Defect in 4H-SiC Epilayers

Robin Karhu, Misagh Ghezellou, and Jawad Ul Hassan*

The origin and the formation mechanism of a surface morphological defect in 4H-SiC epilayers are reported. The defect appears on the surface of an epilayer as an inclined line-like feature at an angle of $\pm 80^\circ$ to the step-flow direction $[11\bar{2}0]$. The defect is confirmed to originate from a threading screw dislocation intersecting the surface and its orientation is controlled by the sign of the Burgers vector of the dislocation. The defect forms through the interaction of local spiral growth associated with threading screw dislocations and step-flow growth related to the substrate offcut. The defect mainly appears in the epilayers grown through chloride-based chemistry, where in situ surface preparation of the substrate is performed in $H_2 + HCl$ at a relatively high temperature.

high density of epitaxial defects, and low charge carrier lifetime, has also been developed in the past few years. Chloride-based chemistry has been shown to significantly improve the epitaxial growth rate to over $100 \mu m h^{-1}$.^[4–8] Using 4° offcut substrates, basal plane dislocations (BPDs) have shown to reduce to less than $0.1 cm^{-2}$ and similar improvements have been made regarding other epitaxial defects such as triangular defects, in-grown stacking faults (SFs),^[9] and other intrinsic defects detrimental for high-power bipolar devices.^[10–14] Considerable improvements in the on-axis homoepitaxy on the Si face of 100 mm-diameter wafers have also shown^[15] to be

an alternative route to obtain thick epilayers free of BPDs that are highly suitable for high-power bipolar devices.^[16]

Surface morphological defects in 4H-SiC epilayers have drawn considerable attention in recent years. Among several types of surface morphological defects, shallow pits,^[17] surface step-bunching,^[18] and short step-bunching^[19,20] are the most common defects. Such defects generally do not lead to the formation of any crystallographic imperfections but only appear as a morphological disturbance in the form of depressions and/or bumps on the surface. Different origins and formation mechanisms have been demonstrated for such defects. For example, surface step-bunching is believed to be a result of locally slowing down of leading steps, allowing for trailing ones to catch them up.^[21] The shallow etch pits are reported to be associated with threading screw dislocations (TSDs) and are formed through the selective etching of TSDs during epitaxial growth and postgrowth oxidation.^[22,23]

Shallow pits and step-bunching have been shown to negatively affect the performance of electronic devices. Recent studies have shown that there is a clear correlation between surface morphological defects and the failure rate of 4H-SiC Schottky barrier diodes (SBDs) and metal–oxide–semiconductor field-effect transistors (MOSFETs).^[24,25] As the negative effect comes from geometrical considerations of the morphological defects,^[26] that is, electric field crowding, most of the surface morphological defects would probably have a similar effect on SBDs and MOSFETs. It is therefore important to understand how and why morphological defects form during the growth and postgrowth processing of 4 H-SiC epitaxial layers.


We report on the origin and the formation mechanism of a surface morphological defect that appears on the surface of 4 H-SiC epilayers as an inclined line at an angle of $\pm 80^\circ$ to the step-flow direction. The surface morphological disturbance created by the defect significantly increases local surface roughness and may influence device characteristics.

1. Introduction

4H-SiC is a wide-bandgap semiconductor with high thermal conductivity, high breakdown electric field, and high saturation electron drift velocity. A combination of such unique physical properties with the possibility of n- and p-type doping during growth and the availability of large-diameter native substrates brings it to the forefront of the family of wide-bandgap semiconductor materials for energy-saving high-power electronics. SiC-based power devices have already made their place in several applications, such as power converters for electric vehicles,^[1] high-efficiency inverters in DC/AC converters for green power generation,^[2] and other industrial high-power applications, saving a significant percentage of electric power.

SiC crystal growth has substantially improved in the past decade and high-quality, large-diameter substrates (up to 200 mm) have already been demonstrated.^[3] Epitaxial growth has also improved and a good understanding of the issues hindering the realization of high-power electronic devices, such as low epitaxial growth rate,

R. Karhu, M. Ghezellou, J. Ul Hassan
Department of Physics, Chemistry, and Biology (IFM)
Linköping University
SE-581 83 Linköping, Sweden
E-mail: jawad.ul-hassan@liu.se

 The ORCID identification number(s) for the author(s) of this article can be found under <https://doi.org/10.1002/pssb.202100512>.

© 2022 The Authors. physica status solidi (b) basic solid state physics published by Wiley-VCH GmbH. This is an open access article under the terms of the Creative Commons Attribution License, which permits use, distribution and reproduction in any medium, provided the original work is properly cited.

DOI: 10.1002/pssb.202100512

2. Results and Discussion

Several epilayers with a thickness ranging from 10 to 100 μm have been grown on 4° off-cut substrates to analyze the general trends in the occurrence of such defects. The gas-phase chemistry and the in situ surface preparation of the substrate are found to strongly affect the occurrence of the inclined line-like defect. The defect has a higher likelihood of occurring if the in situ etching of the substrate is performed in HCl and the growth is performed through chloride-based chemistry at a relatively high temperature ($>1620^\circ\text{C}$) using TCS and propane at C/Si ratio >1 . No formation of such defects has been observed in the epilayer grown using silane and propane as source gasses. Doping type and concentration do not seem to have any role in the formation of inclined line-like defects. Also, growth rate in the range of $10\text{--}100\ \mu\text{m h}^{-1}$ does not seem to influence the density of the defects. The fact that the defect only forms in the epilayers grown using chloride-based chemistry at a relatively high C/Si ratio makes it of high concern because for high-power devices a thick drift layer $>100\ \mu\text{m}$ is needed and the use of chloride-based precursors to achieve high growth rates is inevitable, whereas a larger window for C/Si is necessary to control doping and defects. To discriminate the influence of the substrate, several growth runs were also made on substrates from the same wafer using chloride-based epitaxy and standard epitaxy in two separate growth cells; no inclined line-like defects are observed in epilayer growth through standard epitaxy.

An optical image of a 50 μm -thick epilayer with several inclined line-like defects is given in **Figure 1a**, where some of them are highlighted in arrows marking the starting point and orientation. The defects oriented at $+80^\circ$ to the step-flow direction are highlighted in red arrows, whereas -80° are highlighted in yellow arrows.

The density of the defect is rather high (about $2000\ \text{cm}^{-2}$), does not vary much among different epilayers grown on substrates from different suppliers, and corresponds to a typical density of TSDs in 4 H-SiC substrates. The starting point of the defect is rather sharp, while it fades out gradually as moving away from the starting point, and it is not possible to mark the exact ending point. It grows longer in size with increasing thickness of the epilayer, which is a typical characteristic of an epitaxial defect in the basal plane along the step-flow direction.^[27] The inclined line-like defect, in contrast, grows at an angle of $\pm 80^\circ$ to the step-flow direction and may not be associated with any structural disorder in the basal plane. The surface morphological features of the defect also grow larger with the increasing thickness of the epilayer, and the defect becomes more prominent in the thicker epilayers. An increase in the size of the defect with increasing thickness of the epilayer indicates that the growth of the defect remains active during the entire epitaxial growth process. It is also interesting to notice that $+80^\circ$ defect appears more frequently as compared with -80° . The density of $+80^\circ$ and -80° defects is estimated to be about 70% and 30%, respectively.

An optical image of the same region of the epilayer given in **Figure 1a** but after etching in molten KOH (**Figure 1b**) reveals all kinds of dislocations intersecting the surface of the epilayer with characteristic etch pits.^[28,29] TSDs are visible as relatively large-diameter hexagonal etch pits (inset in **Figure 1b**), whereas threading edge dislocations (TEDs) appear as relatively small-

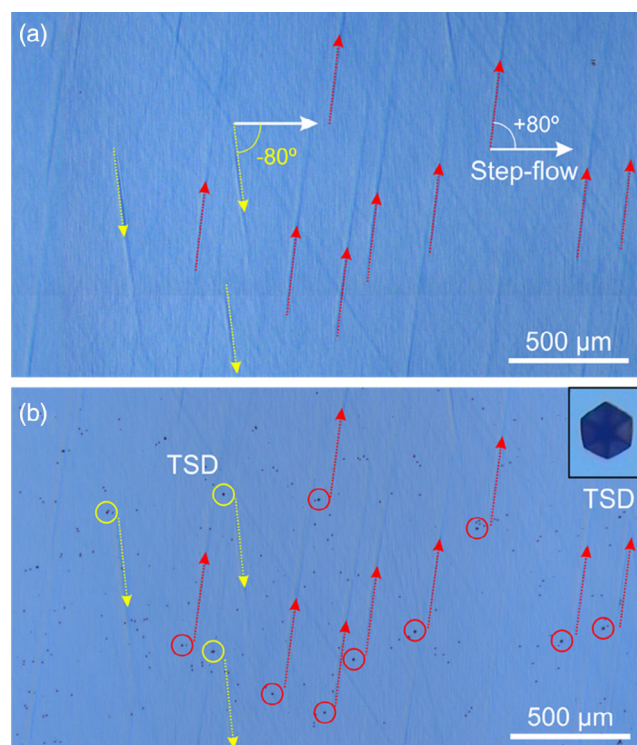


Figure 1. Optical images of a 50 μm -thick-epilayer a) as-grown surface; inclined line-like defects at an angle of $+80^\circ$ and -80° in the step-flow direction are highlighted with red and yellow arrows, respectively, and b) the same region after KOH etching. TSD-related etch pits corresponding to $+80^\circ$ and -80° inclined line-like defects are highlighted in red and yellow circles, respectively. The inset in (b) shows a high-magnification image of the TSD-related hexagonal etch pit.

diameter etch pits. The inclined line-like defect did not show any preferential etching along the line or oval-shaped etch pits at the endpoint of the defect. This indicates that there is no associated SF either in the prismatic or in the basal plane and the defect is a pure surface morphological defect.

A careful analysis of the etched surface reveals the presence of TSD-related etch pits (highlighted in red and yellow circles in **Figure 1b**) in the step-up direction of the starting point of each inclined line-like defect. A pure closed core TSD can have a Burgers vector of either $+1c$ or $-1c$, the so-called right- or left-handed dislocations, respectively. The formation of an inclined line-like defect next to every TSD clearly indicates that it may have originated from TSD and its appearance either at $+80^\circ$ or -80° with respect to the step-flow direction can be a characteristic of the sign of the Burger vector of the associated TSD.

To confirm the correlation of the orientation of inclined line-like defects with the sign of the Burger vector of TSDs, monochromatic synchrotron X-ray topography was performed. X-ray topography in the grazing-incident angle with the \mathbf{g} -vector $[11\bar{2}8]$ allows to determine the sign of the Burgers vector of TSDs through the asymmetric contrast. The contrast originates from the sign of the Burgers vector and the direction of the \mathbf{g} -vector. A detailed study on the assignment of $+1c$ and $-1c$ TSD depending on the orientation of asymmetric contrast is given in the study by Chen et al.^[30] **Figure 2a** shows an optical

image of a 35 μm -thick epilayer with several inclined line-like defects, some of the $+80^\circ$ and -80° defects are highlighted in red and yellow arrows, respectively. The layer was grown using chloride-based chemistry at a growth rate of $35 \mu\text{m h}^{-1}$ with C/Si ratio of 1.2. An X-ray topographic image of the same region of the epilayer with the \mathbf{g} -vector of $[11\bar{2}8]$ is given in Figure 2b, where TEDs appear as small white dots, while TSDs appear as relatively large white dots.^[31] Based on the asymmetric contrast, TSDs with Burgers vector $+1c$ are highlighted in red circles, while TSDs with Burgers vector $-1c$ are highlighted in yellow circles. High-magnification images of $+1c$ and $-1c$ TSDs are also given at the bottom of Figure 2, where the asymmetric contrast is pointed with arrows. A comparison of Figure 2a,b shows a clear one-to-one correlation for $+80^\circ$ inclined line-like defects (red arrows) with $+1c$ -type TSDs and -80° inclined line-like defects (yellow arrows) with $-1c$ -type TSDs. This confirms that 1) TSDs triggered the formation of inclined line-like defects and 2) the sign of Burgers vector determines whether the inclined line-like defect will appear at $+80^\circ$ or -80° in the step-flow direction.

Figure 3a shows an AFM surface topographic image of a section of an inclined line-like defect. The surface line profile of the defect, given in Figure 3b, clearly shows a large dip followed by the ripples which fade out as moving away from the defect in the step-flow direction. The depth of the dip is rather high (40 nm in 50 μm -thick epilayer) and is found to increase with the increasing thickness of the epilayer. The length of an inclined line-like defect in a 50 μm -thick epilayer is estimated to be about 600 μm and probably reflects the strain field around a TSD. This indicates that the screw character of TSDs may have

long-range influence on the surface and continues to oppose the step flow throughout the growth process.

On several occasions, an interaction between inclined line-like defects originating from neighboring TSDs has been also observed. When dislocations have the same sign of the Burgers vector, the associated line-like defects assist each other through overlapping (Figure 4) and as a result, the surface morphological disturbance appears more pronounced. In the case when inclined line-like defects originating from TSDs with opposite signs of the Burger vector intersect each other, at the point of intersection, they cancel each other's effect and stop the growth of defect (Figure 4).

Based on the surface appearance, KOH etching behavior, X-ray topographic measurements, and growth mechanisms, we propose a model of the origin and formation mechanism of the inclined line-like defect, given in a schematic illustration in Figure 5. The screw character of dislocation leads to the formation of the unit-cell height step (1 nm in the case of 4 H-SiC) on the (0001) surface.^[32] During growth, geometrically, the step winds into a hexagonal spiral around the core of dislocation in a direction based on the sign of Burgers vector and leads to so-called spiral growth.^[33] TSDs with Burgers vector $+1c$ lead to a counterclockwise flow, while $-1c$ leads to the clockwise flow of steps in a spiral.^[34] In the case of offcut substrates, the surface is covered with steps and epitaxial growth is driven by step-flow growth which forces the steps to move in the offcut direction.

During growth, in the case of $+1c$ TSD, the step related to TSD is winding counterclockwise (Figure 5a). At the lower side of the image, the offcut-related steps (step-flow growth) and TSD-

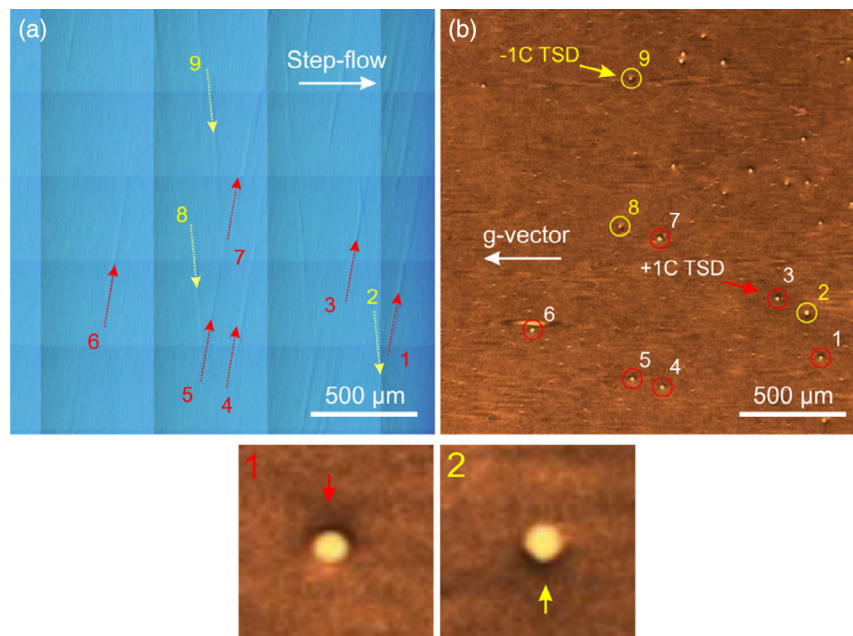


Figure 2. a) Optical image of a 35 μm -thick epilayer with several inclined line-like defects. Some of the $+80^\circ$ and -80° defects are highlighted in red and yellow arrows, respectively. b) Grazing-incident X-ray topographic image from the same region of the epilayer. TSDs' related dots corresponding to the starting point of $+80^\circ$ and -80° inclined line-like defects are highlighted in red and yellow circles, respectively. The defects are numbered from 1–9 to assist the eye in both images. High-magnification X-ray topographic images given at the bottom of the figure show asymmetric contrast of (1) $+1c$ and (2) $-1c$ TSDs corresponding to $+80^\circ$ and -80° inclined line-like defect, respectively.

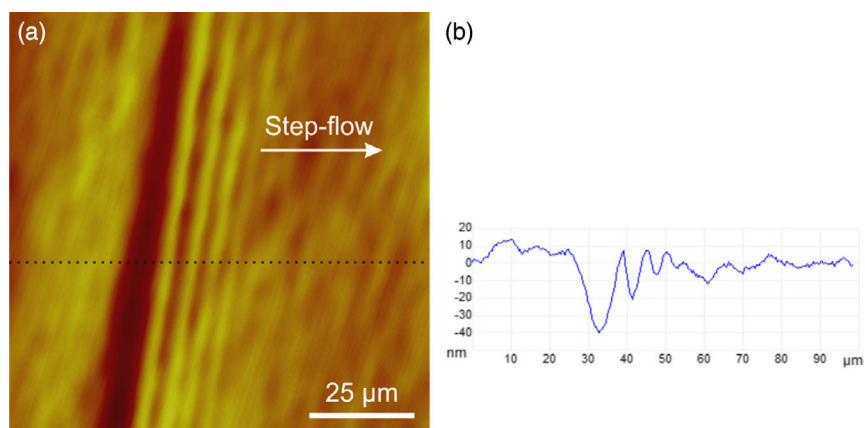


Figure 3. a) AFM surface topographic image of the inclined line-like defect taken from a 50 μm -thick epilayer and b) line profile across the defect. The defect is characterized by a large depression followed by fading ripples.

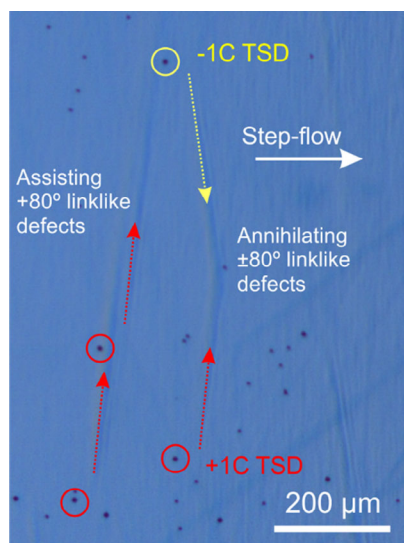


Figure 4. Optical image of a 50 μm -thick epilayer after KOH etching. The red and yellow arrows mark $+80^\circ$ and -80° inclined line-like defect. Corresponding $+1c$ and $-1c$ TSDs are highlighted in red and yellow circles, respectively.

related step (spiral growth) propagate in the same direction. Both growth modes assist each other and hence there is no formation of a surface morphological defect on this side. On the upper side of the same image, the counterclockwise-winding TSD-related step propagates in a direction opposite to the step flow. The local velocities of the spiral and step-flow growth are now in opposite directions. This presents an obstacle in the flow of steps related to step-flow growth and leads to local reduction in the velocity of the steps and allows for the trailing steps to accumulate along a line at $+80^\circ$ to the step-flow direction and hence results in the formation of inclined line-like defects. The spiral step on the other side of the TSD is always moving in the same direction as the step flow, and there is no disturbance on the surface and hence no formation of defect on this side of the TSD. The formation mechanism of the -80° line-like defect in the vicinity of $-1c$ TSD can also be explained in the same way. The appearance of the inclined line-like defect at a few micrometers in the step-down side of the TSD could be due to the dominant step-flow growth, which keeps on pushing it during growth. The defect may have started at the core of TSD, but a continuous push of step flow keeps it moving away from the dislocation. The formation of inclined line-like defects on the 4° offcut surface also indicates that even though growth is dominated by the offcut-related step-flow growth, it is not farfetched to

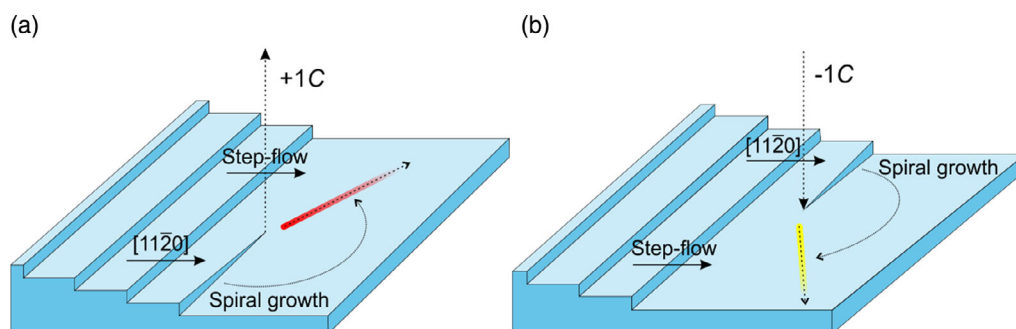


Figure 5. Schematic illustration of the proposed model of the origin and formation mechanism of a) $+80^\circ$ inclined line-like defect originating from a TSD with Burgers vector $+1c$ and b) -80° inclined line-like defect originating from a TSD with Burgers vector $-1c$.

suspect that TSD-related steps can also lead to localized spiral growth around the core of TSDs and interact with the step-flow growth.

We suspect that high-temperature in situ etching of the substrate in $H_2 + HCl$ is relatively aggressive compared to standard in situ etching in H_2 , and surface step-bunching already starts to take place during in situ etching.^[35] This reveals large (0001) terraces on 4° offcut surface and allows for selective etching of TSD and hence the formation of microscopic etch pits with spiral-like features. During the growth process, even though the growth mode is dominant by the step-flow growth, the local growth around TSDs may also takes place through spiral growth. The spiral step moving in a direction opposite to the step-flow growth opposes the flow of steps and leads to the formation of an inclined line-like defect on the surface. The model is further supported by the evidence of the phenomena of “assistance” and “annihilation” of inclined line-like defects originating from neighboring TSDs (Figure 4). The opposition to the step-flow growth is doubled due to the combined effect of the TSDs with a similar sign of the Burger vector and leads to a more pronounced disturbance on the surface, whereas TSDs with opposite signs of the Burger vector, upon interaction, cancel out each other's effect and annihilate the defect.

3. Conclusion

The origin and formation mechanism of a surface morphological defect that appears as an inclined line-like feature on the surface of the 4 H-SiC epilayer are reported. The defect appears at an angle of $\pm 80^\circ$ to the step-flow direction and grows longer with the increasing thickness of the epilayer. In situ etching of the substrate under $H_2 + HCl$ and epitaxial growth at a relatively high temperature through chloride-based epitaxy using propane as C precursor at a relatively high C/Si ratio promote the formation of the inclined line-like defects. No such defects have been observed in epilayers grown under the same conditions using standard chemistry (silane and propane) following the in situ etching of the substrate in H_2 . TSDs in the substrate are found to be the origin of these defects. The defect is formed through the interaction of local spiral growth around TSD and step-flow growth. The sign of the Burgers vector of TSD determines whether the inclined line-like defect will appear at an angle of $+80^\circ$ or -80° to the step-flow direction. The defect is purely surface morphological and does not lead to any structural disorder in the epilayer.

4. Experimental Section

Epitaxial growth was performed in a horizontal hot-wall chemical vapor deposition (CVD) reactor on commercially available nitrogen-doped 4H-SiC substrates with an offcut of 4° toward $[1\bar{1}20]$ direction. The precursors used were trichlorosilane (TCS; $HSiCl_3$) or silane (SiH_4) as a source of Si and propane (C_3H_8) as a source of C, highly diluted in hydrogen. To understand the influence of the in situ surface etching of the substrate and the growth process on the formation of inclined line-like defects, the process parameters were investigated over a wide range. The growth temperature range was $1600\text{--}1650^\circ\text{C}$, C/Si ratio was $0.8\text{--}1.4$, and growth rate was $10\text{--}100\ \mu\text{m h}^{-1}$. The in situ surface preparation of the substrates was performed at growth temperature in $H_2 + HCl$ prior to the growth, while

the influence of the substrate's surface etching time was explored for 1–10 min.

The surface of the epilayers was analyzed through an optical microscope with Nomarski contrast and an atomic force microscope (AFM) in the tapping mode. To reveal any structural defect or dislocation associated with the inclined line-like defect, epilayers were etched in molten KOH at 500°C for 5 min. Monochromatic synchrotron X-ray topography in grazing-incident angle was used to confirm the nature of the defect and determine the sign of the Burgers vector of the associated dislocation. X-ray topography was performed at Spring-8 (Super Photon ring 8 GeV) in Japan using a wavelength of 0.1455 nm.

Acknowledgements

The authors are grateful to Isaho Kamata and Hidekazu Tsuchida at CRIEPI for performing synchrotron X-ray topography. The Swedish Energy Agency *Energimyndigheten* project number 43611-1 is acknowledged for financial support.

Conflict of Interest

The authors declare no conflict of interest.

Data Availability Statement

The data that support the findings of this study are available from the corresponding author upon reasonable request.

Keywords

Burgers vectors, dislocations, epitaxy, spiral growth, step-flow growth, surface morphological defects, X-ray topography

Received: October 6, 2021

Revised: January 10, 2022

Published online:

- [1] J. Lencarski, M. Ricco, V. Monteiro, V. G. Monopoli, *Compat. Pow. Electr.* **2020**, 1, 517.
- [2] Y. Li, Y. Zhang, X. Yuan, L. Zhang, Z. Song, M. Wu, F. Ye, Z. Li, Y. Xu, Z. Wang, *IEEE Trans. Ind. Appl.* **2021**, 57, 5013.
- [3] M. O'Loughlin, A. Burk Jr., D. Tsvetkov, S. Ustin, J. W. Palmour, *Mater. Sci. Forum* **2016**, 858, 167.
- [4] H. Pedersen, S. Leone, A. Henry, F. C. Beyer, V. Darakchieva, E. Janzen, *J. Cryst. Growth* **2007**, 307, 334.
- [5] F. La Via, G. Galvagno, G. Foti, M. Mauceri, S. Leone, G. Pistone, G. Abbondanza, A. Veneroni, M. Masi, G. L. Valente, D. Crippa, *Chem. Vapor Depos.* **2006**, 12, 509.
- [6] J. Hassan, H. Bae, L. Lilja, I. Farkas, I. Kim, P. Stenberg, J. Sun, O. Kordina, J. P. Bergman, S. Ha, E. Janzen, *Mater. Sci. Forum* **2014**, 778–780, 179.
- [7] A. Henry, S. Leone, F. C. Beyer, H. Pedersen, O. Kordina, S. Andersson, E. Janzen, *Physica B* **2012**, 407, 1467.
- [8] H. Tsuchida, I. Kamata, T. Miyazawa, M. Ito, X. Zhang, M. Nagano, *Mater. Sci. Semicond. Process.* **2018**, 78, 2.
- [9] R. E. Stahlbush, B. L. VanMil, R. L. Myers-Ward, K. K. Lew, D. K. Gaskill, C. R. Eddy, *Appl. Phys. Lett.* **2009**, 94, 041916.
- [10] N. T. Son, X. T. Trinh, L. S. Lovlie, B. G. Svensson, K. Kawahara, J. Suda, T. Kimoto, T. Umeda, J. Isoya, T. Makino, T. Ohshima, E. Janzen, *Phys. Rev. Lett.* **2012**, 109.

- [11] L. Lilja, I. D. Booker, J. ul Hassan, E. Janzen, J. P. Bergman, *J. Cryst. Growth* **2013**, 381, 43.
- [12] T. Hiyoshi, T. Kimoto, *Appl. Phys. Express* **2009**, 2, 041101.
- [13] L. Storasta, H. Tsuchida, *Appl. Phys. Lett.* **2007**, 90, 062116.
- [14] T. Miyazawa, T. Tawara, R. Takanashi, H. Tsuchida, *Appl. Phys. Express* **2016**, 9, 111301.
- [15] J. Hassan, R. Karhu, L. Lilja, E. Janzén, *Cryst. Growth Des.* **2019**, 19, 3288.
- [16] A. Salemi, H. Elahipanah, B. Buono, A. Hallen, J. U. Hassan, P. Bergman, G. Malm, C. M. Zetterling, M. Ostling, in *2015 IEEE 27th International Symposium on Power Semiconductor Devices & IC's (ISPSD)*, **2015**, pp. 269–272.
- [17] Y. N. Picard, K. X. Liu, R. E. Stahlbush, M. E. Twigg, *J. Electron. Mater.* **2008**, 37, 655.
- [18] K. Wada, T. Kimoto, K. Nishikawa, H. Matsunami, *J. Cryst. Growth* **2006**, 291, 370.
- [19] K. Masumoto, K. Tamura, C. Kudou, J. Nishio, S. Ito, K. Kojima, T. Ohno, H. Okumura, *J. Cryst. Growth* **2014**, 401, 673.
- [20] K. Masumoto, K. Tamura, C. Kudou, J. Nishio, S. Ito, K. Kojima, T. Ohno, H. Okumura, *J. Cryst. Growth* **2014**, 401, 673.
- [21] T. Kimoto, A. Itoh, H. Matsunami, T. Okano, *J. Appl. Phys.* **1997**, 81, 3494.
- [22] N. Ohtani, *ECS Trans.* **2011**, 41, 253.
- [23] T. Kimoto, *Jpn. J. Appl. Phys.* **2015**, 54, 040103.
- [24] H. Fujiwara, H. Naruoka, M. Konishi, K. Hamada, T. Katsuno, T. Ishikawa, Y. Watanabe, T. Endo, *Appl. Phys. Lett.* **2012**, 100, 242102.
- [25] H. Fujiwara, H. Naruoka, M. Konishi, K. Hamada, T. Katsuno, T. Ishikawa, Y. Watanabe, T. Endo, *Appl. Phys. Lett.* **2012**, 101, 042104.
- [26] J. Sameshima, O. Ishiyama, A. Shimozato, K. Tamura, H. Oshima, T. Yamashita, T. Tanaka, N. Sugiyama, H. Sako, J. Senzaki, H. Matsuhata, M. Kitabatake, *Mater. Sci. Forum* **2013**, 740–742, 745.
- [27] J. Hassan, A. Henry, P. J. McNally, J. P. Bergman, *J. Cryst. Growth* **2010**, 312, 1828.
- [28] A. Ellison, E. Sörman, B. Sundqvist, B. Magnusson, Y. Yang, J. Q. Guo, O. Goue, B. Raghothamachar, M. Dudley, *Mater. Sci. Forum* **2016**, 858, 376.
- [29] M. Syvajarvi, R. Yakimova, E. Janzen, *J. Electrochem. Soc.* **2000**, 147, 3519.
- [30] Y. Chen, M. Dudley, *Appl. Phys. Lett.* **2007**, 91, 141918.
- [31] T. Ohno, H. Yamaguchi, S. Kuroda, K. Kojima, T. Suzuki, K. Arai, *J. Cryst. Growth* **2004**, 260, 209.
- [32] J. Hassan, J. P. Bergman, A. Henry, E. Janzen, *J. Cryst. Growth* **2008**, 310, 4430.
- [33] J. Ul Hassan, R. Karhu, L. Lilja, E. Janzén, *Cryst. Growth Des.* **2019**, 19, 3288.
- [34] Y. N. Picard, M. E. Twigg, *J. Appl. Phys.* **2008**, 104, 124906.
- [35] X. Li, J. Ul Hassan, O. Kordina, E. Janzen, A. Henry, *Mater. Sci. Forum* **2013**, 740–742, 225.